

## Excited State Proton-Transfer Reactions of Coumarin 4 in Protic Solvents

Boiko Cohen and Dan Huppert\*

School of Chemistry, Raymond and Beverly Sackler Faculty of Exact Sciences, Tel-Aviv University, Ramat-Aviv, Tel-Aviv 69978, Israel

Received: February 14, 2001; In Final Form: May 7, 2001

Excited state 7-hydroxy-4-methyl coumarin (4CUOH) has dual photochemical properties. In water, its neutral form (ROH\*) is a strong photoacid and transfers a proton to the solvent with  $pK^* \sim 0$ . It is also a strong photobase capable of accepting a proton from some protic solvents or reacting with excess protons in solution. In this study, we measured the rate and dynamics of the reaction of excited state 4CUOH with excess protons in neat monols and water–glycerol solutions. The reaction shows diffusion-controlled reactivity and fits the Smoluchowski model. The reaction can be formulated by the kinetic scheme  $ROH^* + H^+ \rightarrow ROH_2^{+*}$ , where  $ROH_2^{+*}$  and  $ROH^*$  are the protonated and neutral forms of the photobase, respectively. Nonexponential decay of the  $ROH^*$  fluorescence was observed. We analyzed the experimental data within the framework of the diffusive model. The model predicts that the survival probability depends strongly on both the intrinsic rate constant and the mutual diffusion constant.

### Introduction

The kinetics of many physical, chemical, and biological processes is influenced by diffusion.<sup>1</sup> Electron and hole-trapping processes in semiconductors, acid–base reactions, ion association–dissociation, electron-transfer reactions, and the dynamics of proteins, enzymes, and membranes are common examples of such processes.<sup>1–4</sup>

Many organic compounds<sup>5</sup> become strong acids or bases in the first electronically excited state. Light serves as an ultrafast trigger for proton transfer to and from the solvent. 1-Naphthol, 2-naphthol, and their derivatives undergo an enhancement of acidity when excited to their first electronically excited singlet state.<sup>6</sup> Many photoacids exhibit acid–base equilibrium in their excited state. In these cases, both proton dissociation and recombination occur reversibly on the excited state potential surface.<sup>7–12</sup>

The introduction of relatively large concentrations of moderate bases to the photoacid solution results in direct reaction of the base with the photoacid  $ROH^* + B^- \rightarrow RO^{-*} + BH$ . In recent studies, we measured, using the time-correlated single photon-counting<sup>13,14</sup> and femtosecond pump–probe technique,<sup>14</sup> the direct proton transfer from the excited photoacids, 8-hydroxypyrene-1,3,6-trisulfonate (HPTS) and 2-naphthol-6-sulfonate (2N6S), to acetate in aqueous solution and binary water–glycerol solutions. The reaction rate was measured in the concentration range of 0.5–4 M of sodium acetate (NaAc). We used a diffusive approach to analyze the experimental data. We found good agreement between the Smoluchowski model<sup>15</sup> and the experimental data. The model predicts bimolecular irreversible diffusion-influenced reactions and a nonexponential decay of the survival probability of an excited chromophore.

Coumarin dyes are widely distributed in nature, and some of the derivatives are of great importance in chemistry, biochemistry, and medicine. Chen<sup>16</sup> indicated that 7-hydroxy-4-methyl

coumarin (4CUOH) is a useful indicator for following the pH change induced in the carbonic anhydrase-catalyzed hydration of  $CO_2$ . Many coumarins are naturally fluorescent. In the ground state, hydroxy coumarins in aqueous solution have mild acid–base properties,  $pK_a \sim 7$ . In the excited state, they are much stronger acids—photoacids,  $\Delta pK^* = (pK_a - pK_a^*) \approx 7$ . 4CUOH shows dual photoreactivity in the excited state.<sup>17–19</sup> In its neutral form,  $ROH^*$ , it can transfer a proton to protic solvents. In water, we find that the proton-transfer rate constant is large,  $k_d \sim (20 \text{ ps})^{-1}$ . In monols, it is at least three orders smaller, i.e.,  $k_d < 10^8 \text{ s}^{-1}$ , i.e., smaller than the radiative rate. Hence, this process has a low quantum yield. The excited state 4CUOH can also react with the solvent, SOH, and abstract a proton,  $ROH^* + SOH \rightarrow ROH_2^{+*} + SO^-$ . It reacts much faster with excess protons in solution<sup>17</sup> to form  $ROH_2^{+*}$ . Thus, 4CUOH is also a strong photobase.

In this study, we focus our attention on the photobase reaction of 4CUOH with excess protons in water–glycerol and linear alcohol solutions. We use the Smoluchowski model<sup>7–14</sup> to analyze the experimental data. As will be shown, the model fits the experimental results well.

### Experimental Methods and Data Analysis

7-Hydroxy-4-methyl coumarin (4CUOH, Kodak, >99% chemically pure) was mainly dissolved in methanol, ethanol, propanol, pentanol, and water–glycerol mixtures as well as other solvents. Concentrated  $HClO_4$  (Merck, Darmstadt, 70% in aqueous solution) was added to the alcohol solution. Various solutions with acid concentrations between 0.1 and 1.8 M were used. The water concentration at 1.8 M was  $\sim 4 \text{ M}$ . We found that at 1 M acid concentration, the water only slightly affects the reaction rate. 4CUOH sample concentrations were between  $2 \times 10^{-4}$  and  $5 \times 10^{-4} \text{ M}$ . All chemicals were used without further purification. Steady-state fluorescence spectra of the samples were recorded on an SLM-AMINCO-Bowman 2 luminescence spectrometer and corrected according to manu-

\* To whom correspondence should be addressed. E-mail: huppert@tulip.tau.ac.il. Fax/phone: 972-3-6407012.

facturer specifications. All experiments were performed at room temperature (ca.  $22 \pm 2$  °C).

Time-resolved fluorescence was measured using the time-correlated single-photon-counting (TCSPC) technique. As an excitation source, we used a CW mode-locked Nd:YAG-pumped dye laser (Coherent Nd:YAG Antares and a 702 dye laser) providing a high repetition rate ( $> 1$  MHz) of short pulses (2 ps at full width at half-maximum, fwhm). The TCSPC detection system is based on a Hamamatsu 3809U, photomultiplier, Tennelec 864 TAC, Tennelec 454 discriminator, and a personal computer-based multichannel analyzer (nucleus PCA-II). The overall instrument response was about 50 ps (fwhm). Measurements were taken over a 10 nm spectral width.

### The Diffusive Model

Bimolecular irreversible diffusion-influenced reactions in the pseudo-unimolecular limit when one reactant (say, B) is in excess are the subject of the celebrated “Smoluchowski theory”.<sup>15</sup> At the limit where the donor (A) is static, this theory is exact. It is also an excellent approximation when both donor and acceptor move. The initial decay is faster than exponential because of the excess of B molecules at close proximity to A. As this density approaches its steady-state limit, the reaction becomes exponential, with the ubiquitous diffusion-control rate coefficient,  $k_D$ . This theory has predominantly been applied to fluorescence quenching, but it proved difficult to find conclusive experimental evidence for the predicted initial nonexponential regime in the quenching kinetics. Recently, we showed<sup>13</sup> that the theory fits nonexponential dynamics observed in photoacid–base reactions.

The reaction of accepting an excess proton from the solvent by the excited 4CUOH molecule (ROH\*)



can be described by a diffusive model. According to the Smoluchowski theory,<sup>15</sup> the survival probability of the proton acceptor (here, ROH\*) due to its irreversible reaction with a concentration  $c = [\text{B}]$  of donors is given by

$$S'(t) = \exp(-c \int_0^t k(t') dt') \quad (2)$$

where  $k(t)$  is the time-dependent rate coefficient (or reactive flux at contact) for the donor–acceptor pair

$$k(t) = k_{\text{PT}} p(a, t) \quad (3)$$

The pair (ROH\*/H<sup>+</sup>) density distribution,  $p(r, t)$ , is governed by a Smoluchowski equation

$$\partial p(r, t) / \partial t = D r^{-2} \frac{\partial}{\partial r} r^2 \frac{\partial}{\partial r} p(r, t) \quad (4)$$

with an initial homogeneous distribution and a “radiation” boundary condition at the contact distance ( $r = a$ ), depicting the occurrence of irreversible recombination upon the binary collision.

$$4\pi D a^2 \frac{\partial}{\partial r} p(r, t) |_{r=a} = k_{\text{PT}} p(a, t) \quad (5)$$

There are several input parameters for this model. As customary,  $a$  is taken as 7 Å.<sup>6</sup>  $k_{\text{PT}}$  is the bimolecular rate coefficient which, for 4CUOH in methanol solution, we find in this study to be  $\sim 10^{10} \text{ M}^{-1} \text{ s}^{-1}$ . Both  $k_{\text{PT}}$  and  $a$  did not vary

**TABLE 1: Relevant Parameters for the Proton-Transfer Reaction of 4CUOH in Monols**

[HClO <sub>4</sub> ] (M)	alcohol (%)	$\frac{\Lambda}{\text{equiv}^{-1} \text{ s}^{-1} \text{ cm}^2}$	$D \times 10^{-5}$ (cm <sup>2</sup> s <sup>-1</sup> )	$k_{\text{eff}} \times 10^9$ (s <sup>-1</sup> ) <sup>b</sup>	$k_D \times 10^{10}$ (M <sup>-1</sup> s <sup>-1</sup> ) <sup>c</sup>	$k_{\text{PT}}/k_D$ <sup>d</sup>	$k_{\infty} \times 10^{10}$ (M <sup>-1</sup> s <sup>-1</sup> ) <sup>e</sup>
Methanol							
0.10	99	111	3.30	1.10	1.74	0.62	0.66
0.28	97	99	2.90	1.05	1.52	0.71	0.63
0.53	94	90	2.65	1.00	1.40	0.77	0.61
1.12	90	84	2.47	0.91	1.30	0.83	0.59
Ethanol							
0.10	99	39	1.20	1.00	0.63	1.04	0.32
0.28	96	35	1.02	0.91	0.54	1.22	0.29
0.53	90	36	1.06	0.80	0.56	1.18	0.30
1.12	87	37	1.10	0.77	0.58	1.14	0.31
1.55	82	40	1.20	0.71	0.63	1.04	0.32
Propanol							
0.10	98	14	0.40	0.95	0.21	2.62	0.15
0.28	95	13	0.38	0.83	0.20	2.75	0.14
0.82	87	17	0.50	0.77	0.26	2.08	0.18
1.12	84	18	0.53	0.74	0.28	1.96	0.19
1.55	77	21	0.61	0.67	0.32	1.71	0.20

<sup>a</sup> Conductivity of HCl in water–alcohol mixtures taken from ref 22. <sup>b</sup>  $k_{\text{eff}} = k_f + k_{\text{PT}}^{(1)} + k_{\text{PT}}^{(2)}$  (in the absence of excess protons). <sup>c</sup>  $k_D = 4\pi N^{\circ} D a$ . <sup>d</sup>  $k_{\text{PT}} = 1.08 \times 10^{10}$ ,  $0.66 \times 10^{10}$ , and  $0.55 \times 10^{10} \text{ M}^{-1} \text{ s}^{-1}$  for methanol, ethanol, and propanol, respectively. <sup>e</sup>  $k_{\infty} = (k_{\text{PT}} k_D) / (k_{\text{PT}} + k_D)$ .

with the acid concentration. We have solved eq 4 numerically, using a user-friendly Windows application for spherically symmetric diffusion problems (SSDP, ver. 2.61).<sup>20</sup> The adjustable parameters, varying from solvent to solvent, were  $D$ , the relative photobase–proton diffusion coefficient (Table 1), and the background fluorescence intensity,  $b$  (which influenced only the last part of the decay).

For this particular case of no potential between the reacting particles, it is possible to solve the Debye–Smoluchowski equation (DSE) analytically. Collins and Kimball<sup>21</sup> found an exact expression for the time-dependent rate constant

$$k(t) = \frac{4\pi D a k_{\text{PT}}}{k_{\text{PT}} + 4\pi D a} \left\{ 1 + \frac{k_{\text{PT}}}{4\pi D a} e^{\gamma^2 D t} \text{erfc}[(\gamma^2 D t)^{1/2}] \right\} \quad (6)$$

$\gamma$  is given by

$$\gamma = a^{-1} \left( 1 + \frac{k_{\text{PT}}}{4\pi D a} \right) \quad (7)$$

erfc is the complementary error function.  $k_{\text{PT}}$  is the rate constant of the reaction at contact.

The survival probability of ROH\* with finite lifetime  $\tau_f$  surrounded by an equilibrium distribution of excess protons with initial condition  $S(0) = 1$  is

$$S(t) = \exp(-t/\tau_f - c \int_0^t k(t') dt') \quad (8)$$

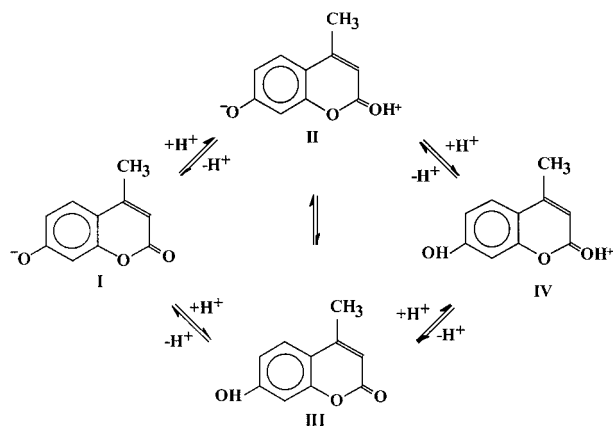
where  $c$  is the concentration of the acid,  $k(t)$  is the time dependent rate constant, given either by the numerical solution<sup>20</sup> or by eq 6,<sup>21</sup> and  $\tau_f$  is the effective ROH\* lifetime.

### Results and Discussion

**Ground State Properties.** Schulman<sup>17</sup> suggested that the possible protolytic equilibria involving the addition and subtraction of protons to the 4CUOH molecule can be described by Scheme 1.

In the ground state at alkaline and neutral pH, species **I**, **II**, and **III** exist. As the acidity is increased, there are two possible

## SCHEME 1

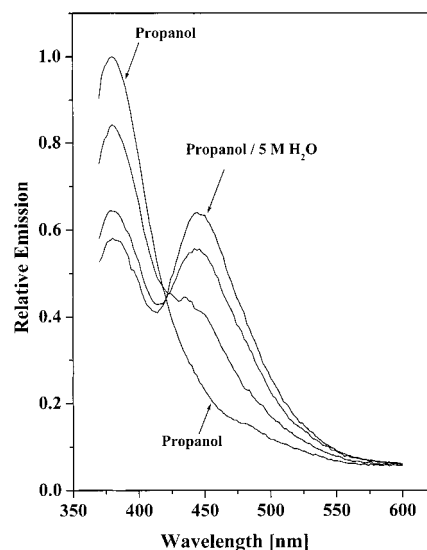


sites of protonation, either at the dissociated phenolic oxygen (leading to the neutral molecule, **III**) or at the carbonyl oxygen (forming the zwitterionic species, **II**). In very strong acid media, a second protonation will lead to the cation, **IV**. The absorption spectra as a function of acidity indicate that **III** is the predominant uncharged species (ROH) in the ground state.<sup>17</sup> The ground state acid–base properties lead to path **I** → **III** → **IV**. At moderate pH ranges, the main process is the acid–base equilibrium,  $\text{ROH} + \text{SOH} \rightleftharpoons \text{RO}^- + \text{SOH}_2^+$ , with an appreciable equilibrium constant,  $\text{p}K_a^1 \sim 7$ .<sup>5</sup> In contrast, the second protonation in the ground state,  $\text{ROH} + \text{SOH}_2^+ \rightleftharpoons \text{ROH}_2^+ + \text{SOH}$ , is unfavorable, and the  $\text{ROH}_2^+$  concentration is very low even at high acid concentrations. The  $\text{p}K_a^2$  of the second protonation reaction is estimated to be  $-5$ .<sup>17</sup> The absorption band maximum of the neutral ROH species is located at 320 nm. In basic solution, the  $\text{RO}^-$  is the predominant species, and its absorption band maximum is at 360 nm. The absorption in strong acidic solution is almost the same as that of the neutral solution because for the second protonation,  $\text{p}K_a^2 \sim -5$ .<sup>17</sup>

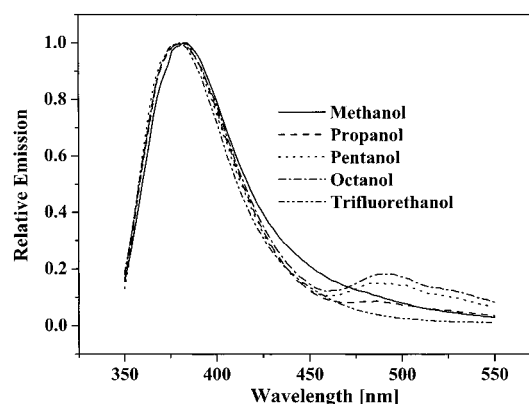
**Excited State Properties.** The steady-state emission of 4CUOH consists of three structureless broad bands, the maxima of which are at 380, 440, and 485 nm. The relative intensity of the emission bands depends on the solution pH and is assigned to the excited state species,  $\text{ROH}^*$  (380 nm, band maximum),  $\text{RO}^{*-}$  (440 nm), and  $\text{ROH}_2^{+*}$  (485 nm) forms. Figure 1 shows the steady-state emission spectrum of water–propanol binary solutions of 4CUOH excited at the maximum of the ROH absorption band. For a large water content in the propanol–water binary solution, the proton-transfer rate to the solvent is large, and therefore, the intensity of the UV emission band ( $\text{ROH}^*$ ; 380 nm) is weak while that of the blue emission band ( $\text{RO}^{*-}$ ; 440 nm) is strong. The isoemissive point is at 415 nm.

Figure 2 shows the steady-state emission of 4CUOH in trifluoroethanol, methanol, *n*-propanol, *n*-pentanol, and *n*-octanol excited at 320 nm, the maximum of the ROH absorption band. In trifluoroethanol, we observe only a single emission band assigned to the  $\text{ROH}^*$  species. In methanol, a slow deprotonation reaction takes place ( $k_d \approx 10^8 \text{ s}^{-1}$ ), and therefore, a trace of the  $\text{RO}^{*-}$  emission can be seen. In the linear monols with a long hydrocarbon chain (*n*-propanol to *n*-octanol), we observe in addition to the  $\text{ROH}^*$  band a second weak emission band. The long wavelength emission band at 485 nm is the same as that of a solution with  $\text{HClO}_4$ . This indicates that the reaction  $\text{ROH}^* + \text{SOH} \rightleftharpoons \text{ROH}_2^{+*} + \text{SO}^-$  is taking place within the excited state lifetime.

Figure 3a shows the time-resolved emission at various wavelengths of 4CUOH in pentanol. At short wavelengths



**Figure 1.** Steady-state emission spectrum of water–propanol binary mixtures of 4CUOH excited at the maximum of the ROH absorption band.



**Figure 2.** Steady-state emission of 4CUOH excited at the ROH absorption band maximum in trifluoroethanol, methanol, propanol, pentanol, and octanol.

(<420 nm), it decays with a lifetime of 1.3 ns, while at long wavelength (>480 nm), a growth in the luminescence curve is seen and the decay time is 4.9 ns. We explain the time-resolved emission data in pentanol as being due to the second protonation reaction. For the short wavelength decay curves, we used the relation  $1/\tau = 1/\tau_{\text{PT}} + 1/\tau_f$  to extract the second protonation rate of pentanol. The excited state lifetime,  $\tau_f$ , of the  $\text{ROH}^*$  form is measured in trifluoroethanol where the proton-transfer reaction does not take place. The luminescence lifetime is 2.1 ns at 370 nm. The derived rate constant for the second protonation is small,  $k_{\text{PT}}^{(2)} = 1/\tau_{\text{PT}} = 2 \times 10^8 \text{ s}^{-1}$ . Because these rates in monols are smaller than  $1/\tau_f \approx 5 \times 10^8 \text{ s}^{-1}$ , we estimate that the error in the determination of  $k_{\text{PT}}^{(2)}$  is  $\pm 30\%$ . The luminescence at 540 nm fits (see Figure 3b) a reaction rate constant of  $2 \times 10^8 \text{ s}^{-1}$ ,  $\text{ROH}^*$  lifetime of 2.1 ns, and a lifetime of the  $\text{ROH}_2^{+*}$  species,  $\tau_f = 4.9$  ns.

Figure 4 shows the time-resolved emissions at various wavelengths of a propanol solution containing 1 M  $\text{HClO}_4$  along with the instrument response function of the time-correlating single-photon-counting system. In the 360–420 nm spectral region ( $\text{ROH}^*$  band), the emission decays at a rate that corresponds to the survival probability of  $\text{ROH}^*$ . At longer wavelengths (>500 nm), the emission's rise time corresponds to the appearance of  $\text{ROH}_2^{+*}$ . At intermediate wavelength, i.e.,

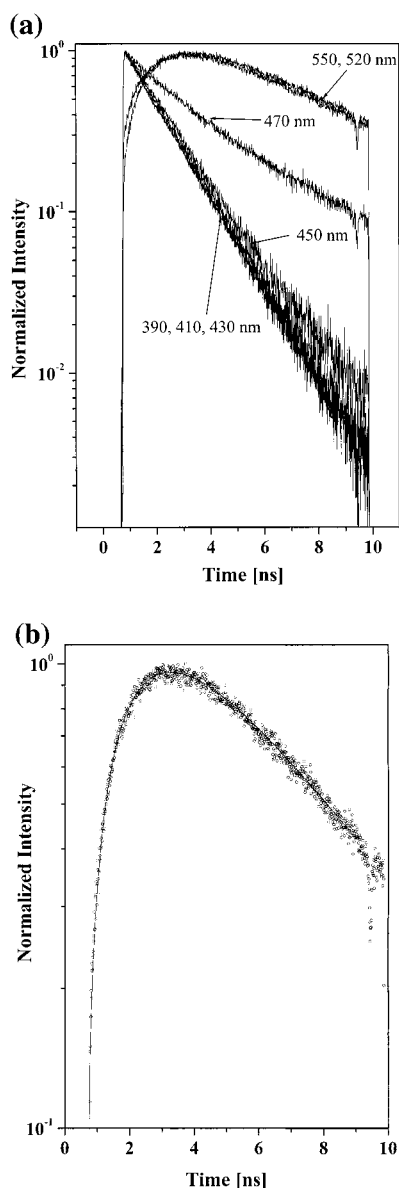


**Figure 3.** Time-resolved emission of 4CUOH (a) at various wavelengths in pentanol and (b) at 540 nm in pentanol along with the fit (solid line) using the parameters given in the text.

460 nm, the emission has two opposite (and almost equal) contributions from both the ROH\* and ROH<sub>2</sub><sup>+</sup>\* bands. The compensation of the two opposite contributions results in an exponential decay with a time constant that corresponds to the excited state lifetime.

Figure 5 shows the time-resolved emission of the ROH\* band measured at 370 nm of 4CUOH–methanol (Figure 5a) and 4CUOH–propanol (Figure 5b) solutions containing various amounts of HClO<sub>4</sub> in the concentration range of 0.1–1.5 M. As the acid concentration increases, the effective lifetime decreases because the photobase–proton reaction rate increases with the HClO<sub>4</sub> concentrations. When the reaction rate of the second protonation of 4CUOH is larger than both the excited state proton-transfer rate to the solvent and the excited state decay rate constant,  $1/\tau_f = (5.7 \text{ ns})^{-1}$ , it strongly affects the effective lifetime of the ROH\*. At HClO<sub>4</sub> concentrations of >0.1 M, the effective lifetimes are shorter. As can be seen, the decay of the luminescence curves at high acid concentrations is nonexponential, and the decay rate depends strongly on the

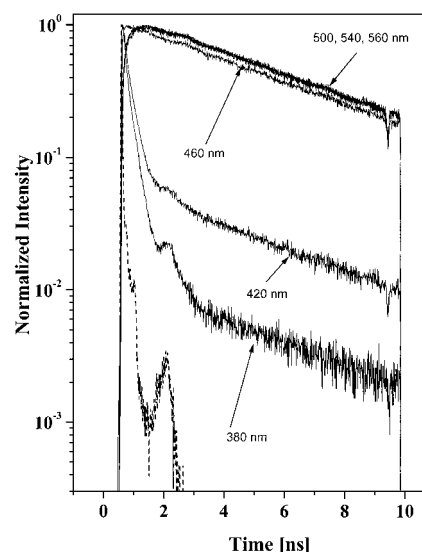


**Figure 4.** Time-resolved emission at various wavelengths of a propanol solution containing 1 M HClO<sub>4</sub>. The normalized instrument response function (IRF) is shown as the dashed curve.

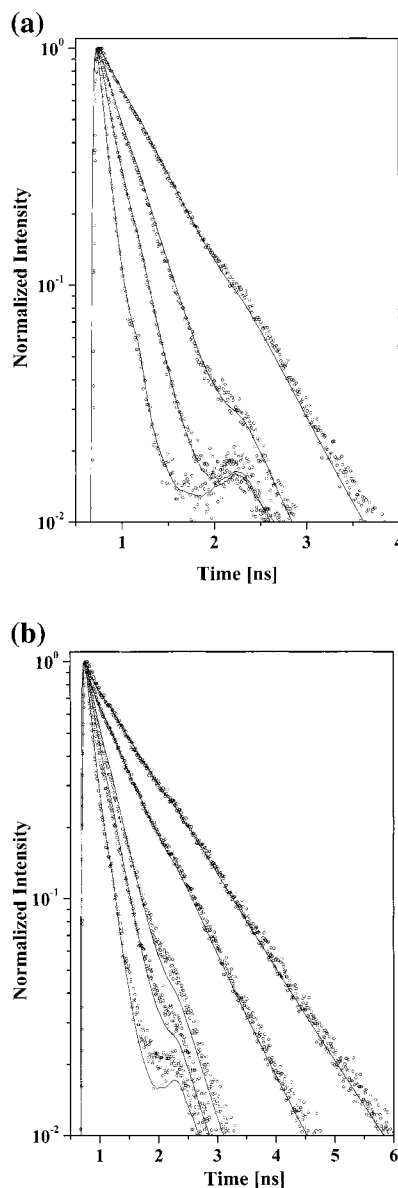
acid concentration. Because the decay of these curves mimics the survival probability of ROH, we fit them using the Smoluchowski model.<sup>15</sup> As can be seen in Figure 5, the fits to the experimental results are very good.

Figure 6a shows the time-resolved emission (dots) measured at 550 nm with the same acid concentration and conditions as those in Figure 5. The growth of the luminescence of these curves corresponds to  $1 - S(t)$ , where  $S(t)$  is the survival probability of ROH\* and  $1 - S(t)$  corresponds to the ROH<sub>2</sub><sup>+</sup>\* concentration due to the reaction ROH\* + H<sup>+</sup> → ROH<sub>2</sub><sup>+</sup>\*. The solid lines in Figure 6a are the computer fit using the Smoluchowski model.

Scheme 1 shows a complex protolytic cycle which in our experiment may result in several possible products and/or intermediates. Excitation of 4CUOH in the ROH form (species III in Scheme 1) in acidic solution might lead to the formation of species II via the intermediate IV. A simpler possibility is that the final product is ROH<sub>2</sub><sup>+</sup>\* (species IV). In the first case, ROH<sub>2</sub><sup>+</sup>\* is the intermediate and the reaction scheme is  $A^* \rightleftharpoons B^* \rightleftharpoons C^*$ . The second case is a single-stage process,  $A^* \rightleftharpoons B^*$ . If the back reaction rate is slow compared to the forward reaction, the reaction kinetics is simple. In this study we used the one-step model to explain our experimental data. To clarify the point of the correctness of our simple model, we conducted time-resolved emission measurements at various wavelengths in the spectral region 360–550 nm. According to the simple model, the fluorescence intensity at a certain wavelength,  $\lambda$ , and time,  $t$ , is given by a superposition of two contributions,

$$I(\lambda, t) \propto S(t)g(\lambda) + (1 - S(t))g'(\lambda). \quad (9)$$

$S(t)$  is the survival probability of ROH\* and  $1 - S(t)$  is the survival probability of ROH<sub>2</sub><sup>+</sup>\*.  $g(\lambda)$  and  $g'(\lambda)$  are the fluorescence line shapes of the ROH\* and ROH<sub>2</sub><sup>+</sup>\*, respectively. Figure 6b shows the fit of the model to the time-resolved measurement at various wavelengths in the spectral range 360–550 nm for a methanol solution of 1 M HClO<sub>4</sub>. As can be seen, the fit is good at all wavelengths. We conclude that the reaction of excess proton with the 4CUOH photobase can be described by a simple one-step process. If intermediates are involved in the reaction, then their concentrations and/or their luminescence



**Figure 5.** Time-resolved emission of the ROH\* form of 4CUOH measured at 370 nm at various HClO<sub>4</sub> concentrations (0.1–1.5 M) along with the computer fit: (a) methanol; (b) propanol.

intensities are small and hence could not be identified in the experimental data.

To enhance the nonexponential tail predicted by the Smoluchowski theory, we decreased the diffusion coefficient by adding a very viscous cosolvent to water, namely, glycerol. When the glycerol content is increased up to a 0.37 mole fraction,  $D$  decreases by a factor of 30 from that in water. Figure 7 shows the time-resolved emission of the ROH\* species of 4CUOH in a water–glycerol mixture of 37 mol % glycerol measured at 370 nm at various HClO<sub>4</sub> concentrations along with the computer fit using the relevant parameters given in Table 2. The nonexponential behavior of the reaction rate is clearly seen.

**The Diffusive Model for Photobase–Proton Reactions.** The main effort in this study was to measure and analyze the decay of the survival probability,  $S(t)$ , of ROH\* in three monols and also in water–glycerol binary mixtures at various excess proton concentrations. The analysis of the experimental data is based on the diffusive model<sup>15,20,21</sup> given in eqs 2–8. Fitting the experimental data required careful treatment. The observed fluorescence intensity of the ROH\* form of 4CUOH,  $I_{\text{obs}}(t)$ , was corrected for a small background,  $b$ . The background is

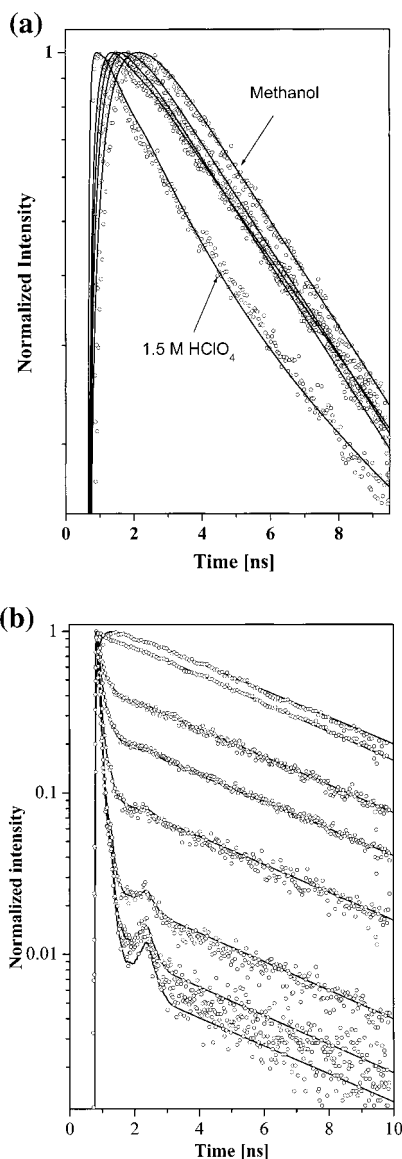


**Figure 6.** Time-resolved emission (dots) along with the computer fits (solid lines) (a) measured at 550 nm in methanol solution with the same acid concentration and conditions as Figure 5a and (b) measured at various wavelengths in methanol solution of 1 M HClO<sub>4</sub>.

attributed either to an overlap of ROH\* and ROH<sub>2</sub><sup>+</sup>\* or to a small degree of dimerization or impurities and degradation of the photobase.  $I_{\text{corr}}(t)$  was subsequently compared with the theoretical survival probability from the Smoluchowski model,  $S(t)$ , of eq 8 after convoluting it with the (independently measured) instrument response function shown in Figure 4. The parameters that control both the rate and the shape of  $S(t)$  are  $k_{\text{PT}}$ ,  $D$ , and  $a$ . The accepted literature value of the contact radius,  $a$ , is taken as 7 Å.<sup>6</sup>

**The Determination of the Diffusion Constant.** The mutual diffusion constant,  $D = D_{\text{H}^+} + D_{\text{ROH}}$ , of each solvent changes because of the presence of a little water when concentrated HClO<sub>4</sub> is added to the sample (concentrated HClO<sub>4</sub> contains 30% water by weight).

The values of  $D_{\text{H}^+}$  at low acid concentration in alcohol–water and water–glycerol solutions were calculated from the conductivity measurements of Erdely-Grüz.<sup>22</sup> These values are given in Tables 1 and 2. The dependence of the mutual diffusion constant,  $D$ , on the acid concentration is large. The diffusion coefficient may be calculated by the Nernst–Einstein equation:<sup>23,24</sup>

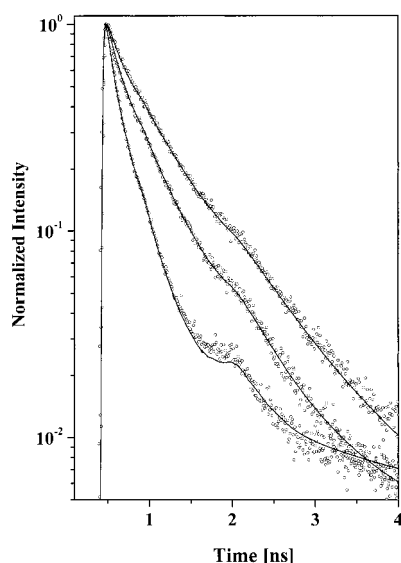


**Figure 7.** Time-resolved emission of the ROH\* species of 4CUOH in a water-glycerol mixture of 37 mol % glycerol, measured at 370 nm at various HClO<sub>4</sub> concentrations. Top to bottom, 0.28, 0.53, and 1.2 M HClO<sub>4</sub>.

**TABLE 2: Relevant Parameters for the Proton-Transfer Reaction of 4CUOH in Water-Glycerol Binary Mixtures**

[HClO <sub>4</sub> ] (M)	glycerol (mol %)	$D \times 10^{-5}$ (cm <sup>2</sup> s <sup>-1</sup> )	$k_D \times 10^{-5}$ (M <sup>-1</sup> s <sup>-1</sup> ) <sup>a</sup>	$k_{PT}/k_D$ <sup>b</sup>	$k_\infty \times 10^{10}$ (M <sup>-1</sup> s <sup>-1</sup> ) <sup>c</sup>
0.28	20	2.60	1.40	4.1	1.13
0.53	20	1.60	0.86	6.7	0.75
1.20	20	1.00	0.54	10.7	0.49
0.28	37	0.89	0.48	10.6	0.43
0.53	37	0.53	0.28	18.2	0.27
1.20	37	0.30	0.16	31.9	0.16

<sup>a</sup>  $k_D = 4\pi N'Da$ . <sup>b</sup>  $k_{PT} = 5.8 \times 10^{10} \text{ M}^{-1} \text{ s}^{-1}$  for 20 mol % glycerol, and  $k_{PT} = 5.1 \times 10^{10} \text{ M}^{-1} \text{ s}^{-1}$  for 37 mol % glycerol. <sup>c</sup>  $k_\infty = (k_{PT}k_D)/(k_{PT} + k_D)$ .

$$D = \frac{RT\lambda}{z^2F^2} \quad (10)$$

Here,  $\lambda$  is the equivalent ionic conductance,  $F$  is the Faraday's constant, and  $z$  is the ionic charge.

In the classical study of electrolyte solutions, ionic mobility at infinite dilution decreases, according to the Kohlrausch law, as  $\sqrt{C}$ . Onsager has derived the following limiting law for  $\lambda$ :<sup>23–25</sup>

$$\lambda = \lambda^0 - (B_1 + B_2\lambda^0)C^{1/2} \quad (11)$$

where  $\lambda^0$  denotes the limiting conductivity at infinite dilution.  $B_1$  and  $B_2$  depend on the temperature, universal constants, and solvent viscosity and dielectric constant.

The retardation of ionic mobility is usually portrayed<sup>23</sup> as a combination of “relaxation” and “electrophoretic” effects, leading to eq 11. While the relevance of both effects is questionable when dealing with protons, the prediction of a larger salt effect on more mobile ions is given by the mobility dependence of the second term in the brackets. HCl conductivity data<sup>25</sup> in aqueous solution approach this limiting behavior at low concentrations. Polarography data<sup>26</sup> tend to agree with those from the conductivity measurements. However, proton tracer diffusion data<sup>27</sup> at 100 mM are significantly lower than the conductivity data. In a previous study<sup>28</sup> on excited state proton geminate recombination in the presence of electrolytes in aqueous solution, a stronger concentration dependence than

predicted by eq 11 was found. The concentration dependence was found to be comparable to the tracer diffusion, and  $D_{H^+}$  was reduced by 25% at 160 mM of NaNO<sub>3</sub> in the solution. In this study, for 0.1 M, the lowest acid concentration used, we calculated  $D$  from the conductivity data.<sup>22</sup> At higher concentrations, we used  $D$  as a free parameter in the computer fit. It affects mainly the intermediate and long times of the decay curve. In the water-glycerol solution,  $D$  decreased by about a factor of 2 in a 1 M acid solution.

**The Intrinsic Proton-Transfer Rate and the Diffusion Rate Constants.** We found that the intrinsic proton capture rate constant from the solution to the photobase,  $k_{PT}$ , depends only slightly on the acid concentration up to  $\sim 1.5$  M but depends strongly on the nature of the solvent. For the linear monols,  $k_{PT}$  was relatively small. In the case of  $k_{PT} > k_D$ , the initial decay of  $S(t)$  is determined by  $k_{PT}$  and at longer times by  $k_D$ . For the lowest acid concentration in methanol, ethanol, and propanol, we found  $k_{PT} = 1.08 \times 10^{10}$ ,  $0.66 \times 10^{10}$ , and  $0.55 \times 10^{10} \text{ M}^{-1} \text{ s}^{-1}$ , respectively. The diffusion-controlled rate constant for these solvents,  $k_D = 4\pi DaN'$ , where  $N' = N_A/1000$  and  $N_A$  is Avogadro's number, is of the same order of magnitude as  $k_{PT}$ . The relevant parameters used in the analysis are given in Table 1. The mutual proton-ROH\* diffusion constants at 0.1 M acid are  $3.3 \times 10^{-5} \text{ cm}^2 \text{ s}^{-1}$  ( $\eta = 0.6$  cP),  $1.2 \times 10^{-5} \text{ cm}^2 \text{ s}^{-1}$  ( $\eta = 1.15$  cP), and  $0.4 \times 10^{-5} \text{ cm}^2 \text{ s}^{-1}$  ( $\eta = 2.4$  cP) for methanol, ethanol, and propanol, respectively. For the lowest acid concentration in methanol, ethanol, and propanol, the diffusion-controlled rate constants are  $1.7 \times 10^{10}$ ,  $0.6 \times 10^{10}$ , and  $0.2 \times 10^{10} \text{ M}^{-1} \text{ s}^{-1}$ , respectively. For 20 and 37 mol % glycerol in water-glycerol mixtures, the proton-transfer rate constants are  $5.8 \times 10^{10}$  and  $5.10 \times 10^{10} \text{ M}^{-1} \text{ s}^{-1}$ , respectively. When  $k_{PT} > 2 \times 10^{10} \text{ M}^{-1} \text{ s}^{-1}$ , the instrument response function of the TCSPC ( $\sim 40$  ps) limits the time resolution and hence the accurate determination of  $k_{PT}$ . We estimate the error in the determination of  $k_{PT}$  in water-glycerol binary mixtures to be  $\sim 30\%$ . We intend to use ultrafast techniques to better resolve the early times of the reaction rate.  $k_D$  for water-glycerol binary mixtures depends on both the glycerol and acid concentrations. The larger the glycerol or the acid concentrations are, the smaller the rate constant is.  $k_D$  changes by almost an order of magnitude from  $k_D = 1.4 \times 10^{10} \text{ M}^{-1} \text{ s}^{-1}$  at 20 mol % of glycerol and 0.28 M acid to  $k_D = 0.16 \times 10^{10} \text{ M}^{-1} \text{ s}^{-1}$  at 37 mol % of glycerol and 1.2 M acid.

#### The Nonexponential Decay of the Survival Probability.

According to the Debye-Smoluchowski diffusion model, when  $k_{PT} \geq k_D$ , the time-dependent rate constant,  $k(t)$ , changes significantly with time which leads to a nonexponential decay of  $S(t)$ . The ratio  $k_{PT}/k_D$  is 0.7, 1.3, and 2.1 for methanol, ethanol, and propanol, respectively. The larger this ratio is, the larger the deviation of  $S(t)$  from a single-exponential decay is. Figure 8 shows the time dependence of  $k(t)$  in methanol, ethanol, and propanol calculated numerically by the SSDP program<sup>20</sup> or by eqs 6 and 7<sup>21</sup> with the relevant parameters of the photobase-excess proton reaction. At  $t = 0$ , it assumes the value  $k_{PT}$ , while the long-time asymptotic expression is given by

$$k_\infty = \lim_{t \rightarrow \infty} k(t) = \frac{4\pi Da k_{PT}}{k_{PT} + 4\pi Da} \quad (12)$$

The lifetime compensated survival probability of ROH,  $S'(t) = S(t) e^{t/\tau_i}$ , is calculated from eq 8 or numerically and is shown for methanol, ethanol, and propanol in Figure 9. For propanol,  $k_{PT}/k_D = 2.1$ , and hence,  $S(t)$  deviates significantly from an exponential decay, while for methanol, this ratio is smaller, 0.7, and therefore,  $S(t)$  deviates much less from an exponential decay.

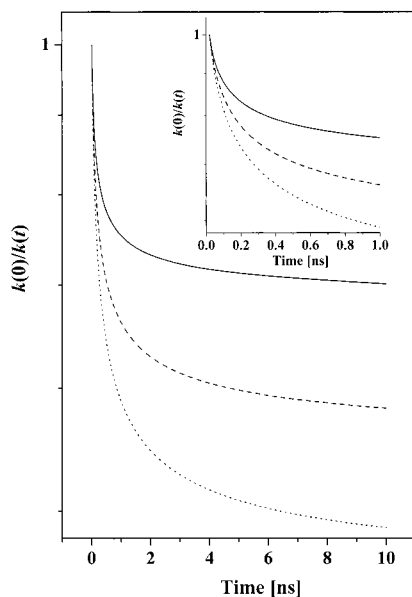


**Figure 8.** Time dependence of  $k(t)$  for methanol (solid line), ethanol (dashed line), and propanol (dotted line) solutions, calculated from eq 6 with the relevant parameters of the photobase–proton reaction.

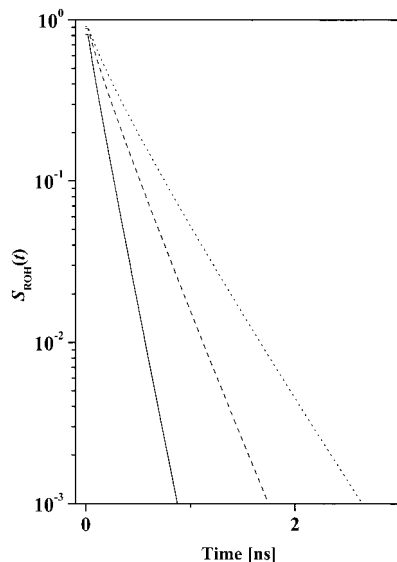


**Figure 9.** The survival probability of ROH,  $S(t)$ , calculated from eq 8 in methanol (solid line), ethanol (dashed line), and propanol (dotted line) solutions at the same acid concentration.

To further enhance the nonexponential tail predicted by the Smoluchowski theory, we measured the reaction in water–glycerol binary mixtures. Figure 10 shows the time dependence of  $S'(t)$  for 37 mol % glycerol in water–glycerol binary mixtures. The nonexponential decay is clearly seen in these samples because  $k_{\text{PT}}/k_{\text{D}}$  ranges from 4.1 to 32 (see Table 2).

### Summary

We have studied the photochemical proton reactivity of 7-hydroxy-4-methyl coumarin (4CUOH) dye in binary water–glycerol mixtures, in water alcohol mixtures, and in neat monols using steady-state and time-resolved emission techniques. In a neutral pH water solution and water-rich alcohol mixtures, the main excited state reaction is proton transfer to the solvent. In neat long-chain monols, the main photochemical reaction is the protonation of the 4CUOH to form  $\text{ROH}_2^{+*}$ . The reaction rate is relatively slow,  $k_{\text{PT}}^{(2)} \sim 2 \times 10^8 \text{ s}^{-1}$ , in pentanol. 4CUOH

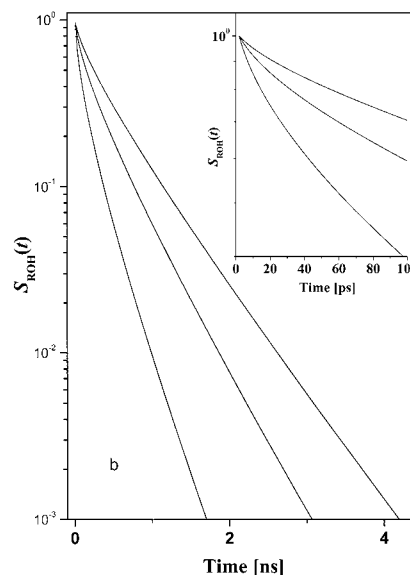


**Figure 10.** The survival probability of ROH\* in water–glycerol binary mixtures of 37 mol % glycerol measured at 370 nm. Top to bottom, the lines represent 0.28, 0.53, and 1.2 M HClO<sub>4</sub>.

reacts efficiently with excess protons in water–glycerol mixtures with an intrinsic rate constant of  $\sim 5 \times 10^{10}$  and  $\sim 10^{10} \text{ M}^{-1} \text{ s}^{-1}$  for methanol and slightly lower rates for longer monols. The reaction can be formulated by the kinetic scheme  $\text{ROH}^* + \text{H}^+ \rightarrow \text{ROH}_2^{+*}$ , where  $\text{ROH}_2^{+*}$  and  $\text{ROH}^*$  are the protonated and neutral forms of the photobase, respectively. Nonexponential decay of the ROH\* fluorescence was observed. We have analyzed the experimental data within the framework of the diffusive model. The model predicts that the survival probability strongly depends on both the intrinsic rate constant and the mutual diffusion constant. We obtained a good fit to the experimental results by the Smoluchowski model.

**Acknowledgment.** We thank Prof. Noam Agmon for his helpful discussion. Our work was partly supported by grants from the Israel Science Foundation and the James–Franck German–Israel program in laser–matter interaction.

### References and Notes

- (1) Rice, S. A. In *Comprehensive Chemical Kinetics*; Bamford, C. H., Tipper, C. F. H., Compton, R. G., Eds.; Elsevier: Amsterdam, 1985; Vol. 25.
- (2) Fleming, G. R. *Chemical Applications of Ultrafast Spectroscopy*; Oxford University Press: New York, 1986.
- (3) Holzwarth, A. R. *Methods Enzymol.* **1995**, *246*, 334.
- (4) Lakowicz, J. R. In *Topics in Fluorescence Spectroscopy*; Lakowicz, J. R., Ed.; Plenum: New York, 1994; Vol. 4.
- (5) Ireland, J. F.; Wyatt, P. A. H. *Adv. Phys. Org. Chem.* **1976**, *12*, 131.
- (6) Weller, A. *Prog. React. Kinet.* **1961**, *1*, 187.
- (7) Pines, E.; Huppert, D. *J. Chem. Phys.* **1986**, *84*, 3576.
- (8) Pines, E.; Huppert, D.; Agmon, N. *J. Chem. Phys.* **1988**, *88*, 5620.
- (9) Agmon, N.; Pines, E.; Huppert, D. *J. Chem. Phys.* **1988**, *88*, 5631.
- (10) Huppert, D.; Pines, E.; Agmon, N. *J. Opt. Soc. Am.* **1990**, *7*, 1500.
- (11) Goldberg, S. Y.; Pines, E.; Huppert, D. *Chem. Phys. Lett.* **1992**, *192*, 77.
- (12) Pines, E.; Magnes, B.-Z.; Lang, M. J.; Fleming, G. R. *Chem. Phys. Lett.* **1997**, *281*, 413.
- (13) Cohen, B.; Huppert, D.; Agmon, N. *J. Am. Chem. Soc.* **2000**, *122*, 9838.
- (14) Genosar, L.; Cohen, B.; Huppert, D. *J. Phys. Chem. A* **2000**, *104*, 6689.
- (15) Von Smoluchowski, M. *Ann. Phys.* **1915**, *48*, 1103.
- (16) Chen, R. F. *Anal. Lett.* **1968**, *1*, 423.

- (17) Yakatan, G. J.; Juneau, R. J.; Schulman, S. G. *Ann. Chem.* **1972**, *44*, 1044.
- (18) Shank, C. V.; Dienes, A.; Trozollo, A. M.; Mayer, J. A. *Appl. Phys. Lett.* **1970**, *10*, 405.
- (19) Bardez, E.; Boutin, P.; Valeur, B. *Chem. Phys. Lett.* **1992**, *191*, 142.
- (20) Krissinel', E. B.; Agmon, N. *J. Comput. Chem.* **1996**, *17*, 1085.
- (21) Collins, F. C.; Kimball, G. E. *J. Colloid Sci.* **1949**, *4*, 425.
- (22) Erdey-Gruz, T.; Lengyel, S. In *Modern Aspects of Electrochemistry*; Bockris, J. O'M., Conway, B. E., Eds.; Plenum: New York, 1964; Vol. 12, pp 1-40.
- (23) Robinson, R. A.; Stokes, R. H. *Electrolyte Solutions*, 2nd ed.; Butterworths: London, 1959.
- (24) Erdey-Gruz, T. *Transport Phenomena in Aqueous Solutions*; Adam Hilger: London, 1974.
- (25) Harned, H. S.; Owen, B. B. *The Physical Chemistry of Electrolytic Solutions*; Reinhold: New York, 1943.
- (26) Roberts, N. K.; Northey, H. L. *J. Chem. Soc., Faraday Trans. 1* **1974**, *70*, 239.
- (27) Woolf, L. A. *J. Phys. Chem.* **1960**, *64*, 481.
- (28) Agmon, N.; Goldberg, S. Y.; Huppert, D. *J. Mol. Liq.* **1995**, *64*, 161.